2016 International Conference on
Unmanned Aircraft Systems (ICUAS)
June 7-10, 2016. Arlington, VA USA

Challenges in Water Stress Quantification Using Small Unmanned Aerial System (sUAS): Lessons from A Growing Season of Almond

Tiebiao Zhao, Brandon Stark, YangQuan Chen*, Andrew L. Ray and David Doll

Abstract— **With water shortages and drought affecting many regions of the world, it becomes urgent to increase water use efficiency (WUE) by optimizing irrigation schedule. Proper irrigation scheduling, which includes integrating of soil moisture monitoring, surface evapotranspiration loss calculation, and plant based measurements is required for high WUE. Stem water potential (SWP) has become one of the more common methods to measure water status. It is, however, labor intensive and time consuming, and adoption has been slow. This study aims to build the link between SWP and canopy normalized difference vegetation index (NDVI) based on aerial multi-spectral images and ground-truth measurement of an almond orchard. Data suggests that the correlation between SWP and canopy NDVI can be improved by tuning canopy NDVI threshold, as indicated by the coefficient of determination (R^2). Also, NDVI shows good correlation with SWP in different growing stages—fruit development and post-harvest. Finally, it is demonstrated canopy NDVI distribution from different missions are significantly different, even if the interval between two flights is less than one hour. This poses the challenge that further calibration is needed to conduct quantitative measurement in long flight missions. Meanwhile, quantitative consideration of characteristic of bi-directional reflectance distribution function makes it necessary to obtain stable performance of canopy NDVI.**

Index Terms— **small unmanned aerial system (sUAS), canopy normalized difference vegetation index (NDVI), water stress detection, stem water potential (SWP)**

I. Introduction

Water is one of the the major constraints in agriculture worldwide and water scarcity is a top problem worldwide[1]. Plants water stress occurs when evaporative demand exceeds the water supply from the soil [2]. Water stress causes stomata closure and reduced uptake of carbon dioxide, leading to diminished crop growth [3]. Almond is no exception, and water stress results in serious yield losses [4], [5], [6], [7]. These losses occur due to a reduction of kernal size and number. Furthermore, stress timing can compound lossess by affecting future crops by impacting floral bud development [7].

Irrigation scheduling is critical in applying the proper amount of water at the right time. Proper scheduling requires taking into account soil moisture status, evaporative demand, and plant water status [5]. Within plant stress monitoring, it has been proven that SWP is a useful index in many fruit tree species and is correlated with short- and medium-term plant response to stress [8]. Detailed guidelines for irrigation scheduling were developed by linking SWP to levels of stress [9], [10]. However, SWP measurement is very labor intensive and time consuming. SWP must occur either during pre-dawn or within 2 hours post solar noon, and requires about 3-5 minutes per sample [10]. This limites the number of samples that can be measured in a given day, making it difficult to measure large fields or conduct a detailed analysis.

Remote sensing has the capability to conduct the real-time measurement over a large scale. Traditional remote sensing platforms like satellites and aircraft are limited by high cost or low resolution, and sometimes affected by weather conditions. Recently, with the remarkable development of small unmanned vehicle systems(sUAS) and imaging sensors, images can be developed with a lower cost, higher spatial resolution and more flexible timing. This spurns considerable research on applications of sUAS in agriculture [11]. A limited amount of research on water stress monitoring using sUAS have been published [12], [13], [14], [15], [16], [17], [18], which shows positive correlation between reflectance indices to water stress indicator—SWP. By far, to date, thermal indices have shown the best correlation with SWP [13], [14]. In these studies, the physiological indicator of stress (PRI) correlated well with canopy temperature ($R^2 = 0.69$) while the region of interest was constrained by NDVI between 0.76 and 0.78 [12]. With NDVI, the relationship with SWP had coefficient of determination up to $R^2 = 0.68$ at the row level [13], whereas at the crown level, NDVI showed weaker sensitivity with SWP ($R^2 = 0.24$) [5]. These two studies utilized images with a spatial resolution 10 and 40 cm/pixel taken once in the growing season.

Enabled by an unmanned aerial vehicle (UAV) installed with a low-cost multi-spectral camera, the goal of this study was to assess the water status at the individual tree level with higher resolution image (1.87 cm) with a more frequent visitation, contrasting studies conducted at the region level [13], row level [13] or crown level [5] and one visit within a growing season. Zhao *et al.* showed [19] that the linear relationship between canopy NDVI and SWP is weak when all the measurements from different weeks are analyzed together. In this study, we focus on the measurements from an individual mission within a short time to minimize the influence of solar motion and canopy structure changes. The relationship between SWP and canopy NDVI was discussed under different NDVI threshold, different growing stages and different time around solar noon.

Tiebiao Zhao, Brandon Stark,and YangQuan Chen are with Mechatronics, Embedded Systems and Automation Lab, University of California, Merced, CA 95343, USA. Email: (tzhao3, bstark2, ychen53@ucmerced.edu). Andrew Ray and David Doll are with University of California, Cooperative Extension (UCCE) Merced County, 2145 Wardrobe Avenue, Merced, CA 95341-6445.

*Corresponding author. Email: ychen53@ucmerced.edu, T: 209-228-4672, F: 209-228-4047, W: http://mechatronics.ucmerced.edu

978-1-4673-9333-1/16/$31.00 ©2016 IEEE

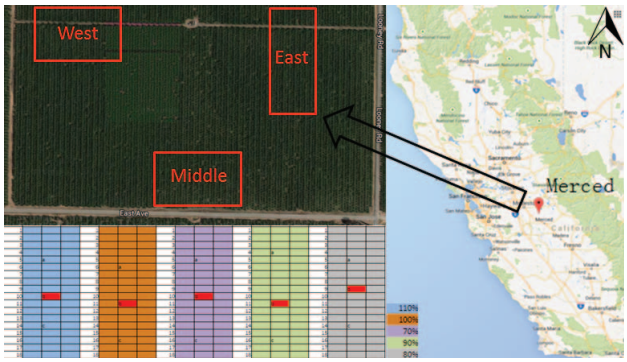

Fig. 1. Overview of the study site in Looney, Merced

II. Materials and Methods

A. sUAS and payload description

The sUAS used in this study was built using DIY Quadkit (3DRobotics, Berkeley, USA), modified to carry a single camera payload for agriculture applications. One COTS (Commercial-off-the-shelve) camera (ELPH110HS, Canon, Japan) was flown from August,2014 to October, 2015, which is configured to detect three bands near-infrared (NIR), green, blue (RGB). The ELPH110HS has a resolution of 4608×3459 pixels with 24 bit radiometric resolution and has a focal length 4.3mm.

The RGB (ELPH110HS, Canon, Japan) camera is converted to the NIR camera by LDP, LLC, USA and its band sets are centered at 430nm, 530nm and 700 nm.

The camera supports Cannon Hack Development Kit (CHDK), which enables the autopilot to trigger cameras as the script programmed, and hence synchronizes the image with GPS and attitude log from the plane. Flight campaigns were conducted around noon at 60m altitude, yielding a ground spatial resolution of 1.87cm.

The raw data digital number (DN) value is converted to reflectance by an empirical method [20]. Before the flight, an image of color checker was taken, where the reflectance of dark (DN_D) and white (DN_W) reference spots are 0 and 0.9 respectively. Then a DN value can be converted to a reflectance using

$$\rho_\lambda = \frac{DN - DN_D}{DN_W - DN_D}. \tag{1}$$

B. Study site

This work was conducted in a mature, commercial almond (Prunus dulcis) orchard in Ballico, Merced County, California (37.493498°N, -120.634914°W). Three varieties of Nonpareil, Carmel, and Monterey were planted on Lovell peach rootstock 16 years ago, spaced at 5.5 m×6.1m. The soil is composed of Rocklin loam and Greenfield sandy. The climate in the region is Mediterranean, characterized by wet, cool winters with a rainy season and hot, dry summers. Records show that its average annual extreme low temperature range from 25° to 30° (F) [21]. Five treatments were carried out in different plots, with the amount of irrigation water equivalent from 70% to 110% of crop evapotranspiration (ET_c), with each treatment increasing 10%. Established in an randomized complete block design, each treatment was replicated in three blocks: middle, west and east block. Each plot is composed of three lines with 18 trees each and a buffer row between treatments (Fig. 1). Crop evapotranspiration was calculated according to Food and Agriculture Orgination (FAO) method [22].

$$ET_c = K_c * ET_o, \tag{2}$$

where ET_o is the evapotranspiration rate of a reference surface under optimum treatment and certain climatic conditions, and K_c crop coefficient is defined as the ratio ET_c/ET_o. K_c utilized in this study was developed in California [7].

C. Field measurement

To determine the effects of irrigation treatments on tree water stress, midday stem water potential (SWP) is measured using a pressure chamber (PMS Instrument Model 600, Oregon, USA) following standard procedures [23]. In 2014, one sample tree in the middle of each plot was measured, five measurements in each block, and in total 15 sample measurements across the trial (middle, west and east). These sample trees were measured once a week from July 31st, 2014 to October 2nd, 2014. The layout of sample trees is shown in Fig. 1, where the sample trees are marked with red. SWP was measured simultaneously as the flight campaigns.

All of the obtained aerial images were stitched together to generate the overall mosaic in Photoscan (AgiSoft LLC, Russia), then the measured trees were cropped manually from the single frame by referring the mosaic, where the sample trees were labeled with the markers. Only the image in the most nadir footprint was considered for further processing.

$$NDVI = \frac{\rho_{NIR} - \rho_B}{\rho_{NIR} + \rho_B}. \tag{3}$$

In this paper, NDVI is calculated following the method (3), where the blue band is used instead of red band, ρ_{NIR} stands for the reflectance of object in NIR band and ρ_B stands for the reflectance in blue band. This is reasonable because the imager was only 60 m above the ground and the atmosphere scattering would not have a significant effect on the blue band. Further, the technique generates better registration accuracy from the optical Bayer filter between the NIR and the blue bands than the method using ground control points.

It is very critical to take pictures of the color checker immediately prior to the flight campaign, otherwise the solar angle and light intensity will change and the conversion will not be accurate. The DN of dark spot and white spot are determined by the point located in the central part of its histogram.

III. Results and Discussions

A. Shade tuning

In citrus, Stagakis et al. [24] classified the image into five objects, sunlit crown, shaded crown, sunlit soil and crown

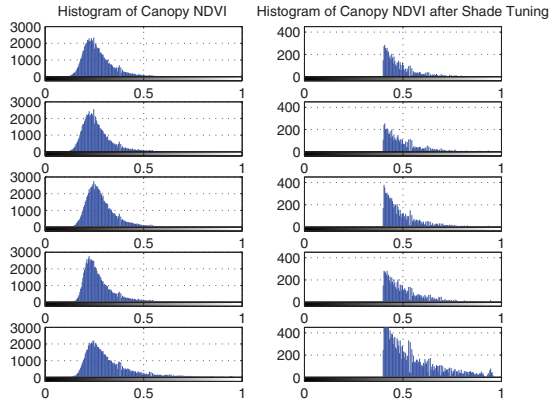

Fig. 2. Distribution of canopy NDVI under different NDVI threshold

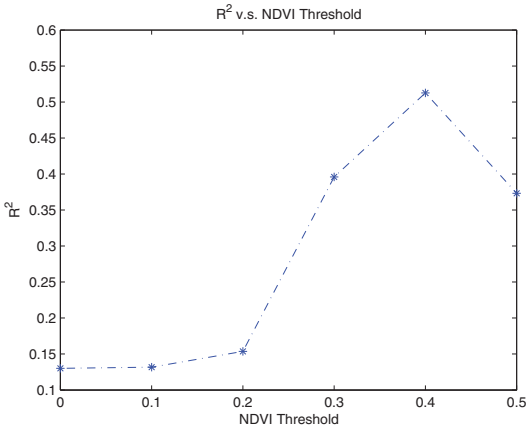

Fig. 3. Effects of NDVI threshold on R^2

edges based on the spectral signatures with the spatial resolution of 30 cm/pixel. It suggested that separation of shaded pixels does not improve the sensitivity to water stress in citrus. Inspired by the work [19], we hypothesis that shaded pixels do not indicate water stress as much as sunlit parts and averaging them together will reduce the relationship between canopy NDVI and SWP. In addition, though all the images taken from different weeks are calibrated with color checker, the solar motion plus canopy growth could cause significant changes between two missions. In order limit these disturbances, we analyze the relationship between vegetation index and SWP with the data collected within one mission.

For each image of the individual tree, first the soil around the canopy was cut away. Then only the region with the NDVI in certain range was recognized as region of interest of the canopy. Finally, canopy NDVI is obtained by averaging these pixels. Experiments show that NDVI upper bound will not help to improve the sensitivity, whereas the lower bound (denoted as $NDVI_{Th}$) could improve the relationship significantly sometimes.

Taking the flight over west block on September 11th, 2014 as an example, the distributions of canopy NDVI of five sample trees are shown in the left side of Fig. 2. Unlike the bimodal histogram of NDVI found in [13] for an entire plot with spatial resolution of 10 cm/pixel, the distribution of canopy NDVI here is unimodal. The right side of Fig. 2 shows the distribution of canopy NDVI after removing the pixels of NDVI lower than 0.4, where the x axis is NDVI, and the y axis is the number of pixels with certain NDVI. Fig. 3 shows the effects of $NDVI_{Th}$ on R^2, where R^2 increases as $NDVI_{Th}$ is increased in the range of 0 to 0.4, and decreases when $NDVI_{Th}$ is increased in the range of higher than 0.4. Maximum R^2 is obtained when $NDVI_{Th}$ is 0.4. The linear relationship between canopy NDVI and SWP is improved from $R^2 = 0.13$ to $R^2 = 0.51$ (Fig. 3).

B. NDVI performance in different growing stages

We also analyzed the relationship in different growing stages, in fruit development and after harvest. The almond hull began to split and allowing it to dry [25] from July to early August. The almond was harvested by the end of September, and leaves started to fall in October. By tuning $NDVI_{Th}$, we have the relationship between canopy NDVI and SWP of $R^2 = 0.7$ and $R^2 = 0.66$ (Fig. 4).

C. Effects of solar motion on canopy NDVI distribution

Then we tried to analyze the relationship using images collected in three mission over three different blocks. In September 4th, 2014, three mission were conducted at 1:03 PM in middle block, 1:45 PM in west block and 2:27 PM in east block. Tests of equality of distribution within these 15 trees are conducted using two sample Kolmogorov-Smirnov test (Matlab2015b, Massachusetts, USA), with null hypothesis that data sample $x1$ and $x2$ are from the same continuous distribution. The result is 1 if test reject the null hypothesis at 1% significance level, and 0 otherwise. Test results indicate that the distributions of canopy NDVI within one block are similar, whereas they are significantly different between two blocks. Table I lists test result between 15 trees in the three blocks, where 'M','W','E' stand for middle block, west block and east block and five trees in each block are numbered from 1 to 5. Therefore, correlation analysis should be made within one mission rather than three missions. It suggests that block-level relationship is more robust, as shown in Fig. 5, where the overall fitting is on the left, and individual block fitting on the right with optimal $NDVI_{Th}$ of 0.1, 0.2 and 0.3 respectively.

IV. Conclusion

The prediction based on canopy NDVI correlates well with SWP, which suggests an alternative method to monitor crop water stress. The canopy NDVI will decrease as the trees are experiencing higher water stress. However, we discovered in this paper that, not all the pixels within the canopy indicate or inform the water stress. This could be explained by the possibility that the pixels with low NDVI are either not leaves, or leaves not illuminated directly by the sun. Therefore, separation of these pixels by tuning the lower NDVI bound or threshold helps optimizing the relationship between canopy NDVI and SWP. Relationships before and

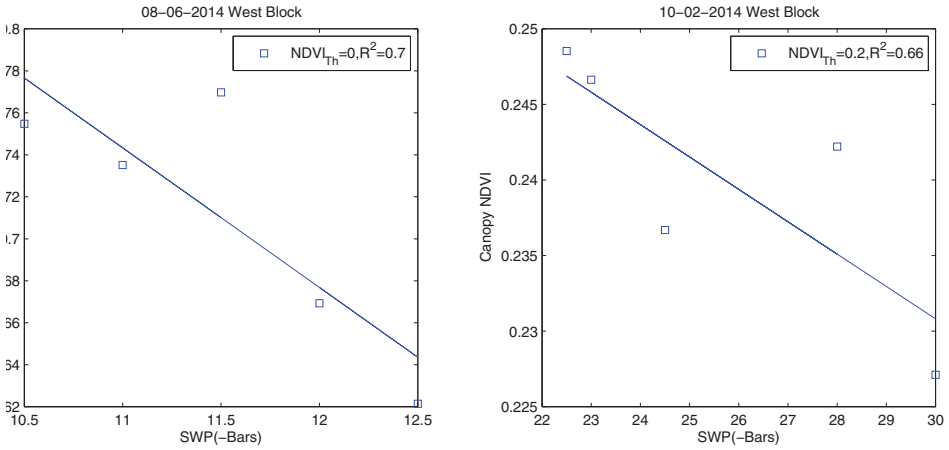

Fig. 4. Relationship between canopy NDVI and SWP in different growing stages

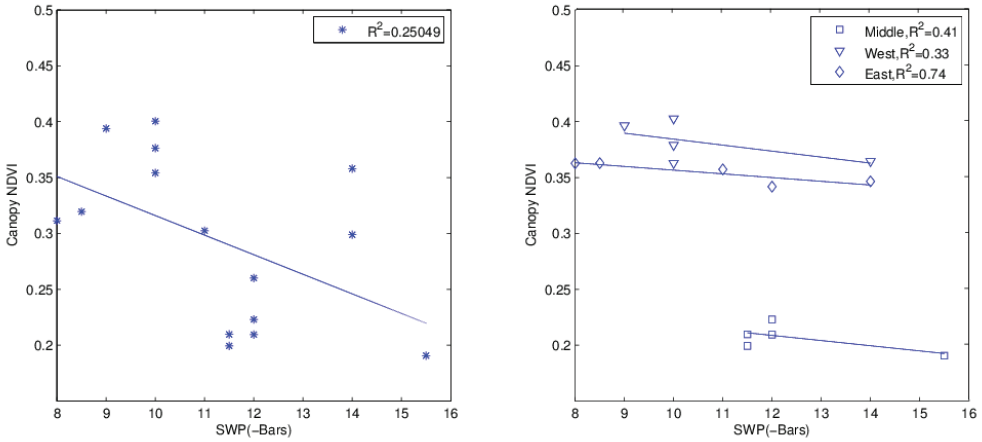

Fig. 5. Relationship between canopy NDVI and SWP in the range of three missions and one mission

after harvest show that canopy NDVI is working well in different growing stages.

This work highlights effects of solar motion and the associated challenges of applying canopy NDVI over a long time. Even a one hour interval will cause a significant change in the distribution. This change happens in the fundamentally physical level regarding canopy spectral response to the illumination of sunlight. Calibration based on color panel

TABLE I

TESTS OF EQUALITY OF DISTRIBUTION WITHIN 15 TREES IN THREE CONSECUTIVE MISSIONS

	M1	M2	M3	M4	M5	W1	W2	W3	W4	W5	E1	E2	E3	E4	E5
M1	0	0	0	0	0	1	1	1	1	1	1	1	1	1	1
M2	0	0	0	0	0	1	1	1	1	1	1	1	1	1	1
M3	0	0	0	0	0	1	1	1	1	1	1	1	1	1	1
M4	0	0	0	0	0	1	1	1	1	1	1	1	1	1	1
M5	0	0	0	0	0	1	1	1	1	1	1	1	1	1	1
W1	1	1	1	1	1	0	0	0	0	0	1	1	1	1	1
W2	1	1	1	1	1	0	0	0	0	0	1	1	1	1	1
W3	1	1	1	1	1	0	0	0	0	0	1	1	1	1	1
W4	1	1	1	1	1	0	0	0	0	0	1	1	1	1	1
W5	1	1	1	1	1	0	0	0	0	0	1	1	1	1	1
E1	1	1	1	1	1	1	1	1	1	1	0	0	0	0	0
E2	1	1	1	1	1	1	1	1	1	1	0	0	0	0	0
E3	1	1	1	1	1	1	1	1	1	1	0	0	0	0	0
E4	1	1	1	1	1	1	1	1	1	1	0	0	0	0	0
E5	1	1	1	1	1	1	1	1	1	1	0	0	0	0	0

does not apply to this disturbance, which matches with the result in [26]. As a result, only images taken within short time range are comparable after calibration with color panel. Images taken in different times will cause different distribution of canopy NDVI, and the analysis by putting them together will not generate good correlation relationship if no advanced corrections adopted.

Another challenging issue is the characteristics of bi-directional reflectance distribution function (BRDF). Even though we conducted the relationship analysis using the images collected in one short flight, the performance was inconsistent. The coefficient of determination R^2 in west block in September 4th was as low as 0.33. This could be caused by BRDF effects. Considering the images of sample trees were manually cropped from each big frame as well as payload vibration impacting resolution, it was very hard to make sure these images were accurately in the nadir shooting range. Accurate BRDF calibration in low-altitude, high-resolution remote sensing is needed to have more consistent correlation relationship and less subjective interference.

ACKNOWLEDGMENT

This work is supported in part by UC ANR Competitive Grant Award No. 13-2628 (2014-2019) entitled "Evaluating and extending the use of small, multi-rotor unmanned aerial vehicles (UAV's) as a crop monitoring tool."

The authors would like to thank Larry Burrow for lending his expertise in almond orchard. Thanks go to the MESA Lab Scientific Data Drone crew members Ph.D. student Brendan Smith and Undergraduate Researchers Yoni Shchemelinin and Andreas Anderson for contributions in conducting flight missions in the 2014 growing season.

REFERENCES

[1] Mesfin M. Mekonnen and Arjen Y. Hoekstra, "Four billion people facing severe water scarcity," *Science Advances*, vol. 2, no. 2, pp. e1500323, 2016.

[2] R. O. Slayter et al., "Plant-water relationships.," *Plant-Water Relationships.*, 1967.

[3] Hans-Eric Nilsson, "Remote sensing and image analysis in plant pathology," *Canadian Journal of Plant Pathology*, vol. 17, no. 2, pp. 154–166, 1995.

[4] David Doll, "Impact of deficit irrigation on almond kernels," Website, 2014, http://www.thealmonddoctor.com.

[5] Pasquale Steduto, Theodore C. Hsiao, Dirk Raes, and Elias Fereres, *Crop yield response to water*, Food and Agriculture Organization of the United Nations Rome, 2012.

[6] K. Shackel, J. Edstrom, A. Fulton, Br Lampinen, L. Schwankl, A. Olivos, W. Stewart, S. Cutter, S. Metcalf, P. Nicolosi, et al., "Drought survival strategies for established almond orchards on shallow soil," *Modesto, CA*, vol. 2012, 2011.

[7] David Doll and Kenneth Shackel, "Drought tip: Drought management for California almonds," ANR Publication 8515, 2015.

[8] Kenneth A. Shackel, H. Ahmadi, W. Biasi, R. Buchner, D. Goldhamer, S. Gurusinghe, J. Hasey, D. Kester, B. Krueger, B. Lampinen, et al., "Plant water status as an index of irrigation need in deciduous fruit trees," *HortTechnology*, vol. 7, no. 1, pp. 23–29, 1997.

[9] A. Fulton, R. Buchner, J. Grant, T. Prichard, B. Lampinen, L. Schwank, and K. Shackel, "Tentative guidelines for interpreting pressure chamber readings(midday stem water potential-SWP) in walnut, almond, and dried plum," Tech. Rep., 2007.

[10] B. Lampinen, S. Sibbett, W. Olson, and K. Shackel, "The relation of midday stem water potential to the growth and physiology of fruit trees under water limited conditions," in *III International Symposium on Irrigation of Horticultural Crops 537*, 1999, pp. 425–430.

[11] Chunhua Zhang and John M. Kovacs, "The application of small unmanned aerial systems for precision agriculture: a review," *Precision Agriculture*, vol. 13, no. 6, pp. 693–712, 2012.

[12] Jose AJ Berni, Pablo J Zarco-Tejada, Lola Suárez, and Elias Fereres, "Thermal and narrowband multispectral remote sensing for vegetation monitoring from an unmanned aerial vehicle," *Geoscience and Remote Sensing, IEEE Transactions on*, vol. 47, no. 3, pp. 722–738, 2009.

[13] Javier Baluja, Maria P. Diago, Pedro Balda, Roberto Zorer, Franco Meggio, Fermin Morales, and Javier Tardaguila, "Assessment of vineyard water status variability by thermal and multispectral imagery using an unmanned aerial vehicle (UAV)," *Irrigation Science*, vol. 30, no. 6, pp. 511–522, 2012.

[14] Victoria Gonzalez-Dugo, P. Zarco-Tejada, José A. J. Berni, L. Suárez, D. Goldhamer, and E. Fereres, "Almond tree canopy temperature reveals intra-crown variability that is water stress-dependent," *Agricultural and Forest Meteorology*, vol. 154, pp. 156–165, 2012.

[15] Pablo J. Zarco-Tejada, Victoria González-Dugo, L. E. Williams, L. Suárez, José A. J. Berni, D. Goldhamer, and E. Fereres, "A PRI-based water stress index combining structural and chlorophyll effects: Assessment using diurnal narrow-band airborne imagery and the CWSI thermal index," *Remote Sensing of Environment*, vol. 138, pp. 38–50, 2013.

[16] Victoria Gonzalez-Dugo, P. Zarco-Tejada, E. Nicolás, P. A. Nortes, J. J. Alarcón, D. S. Intrigliolo, and E. Fereres, "Using high resolution UAV thermal imagery to assess the variability in the water status of five fruit tree species within a commercial orchard," *Precision Agriculture*, vol. 14, no. 6, pp. 660–678, 2013.

[17] J Gago, S. Martorell, M. Tomás, A. Pou, B. Millán, J. Ramón, M Ruiz, R. Sánchez, J. Galmés, MÀ Conesa, et al., "High-resolution aerial thermal imagery for plant water status assessment in vineyards using a multicopter-RPAS," in *Proceedings of*, 2013.

[18] Pablo J. Zarco-Tejada, M. L. Guillén-Climent, Rocío Hernández-Clemente, A. Catalina, M. R. González, and P. Martín, "Estimating leaf carotenoid content in vineyards using high resolution hyperspectral imagery acquired from an unmanned aerial vehicle (UAV)," *Agricultural and Forest Meteorology*, vol. 171, pp. 281–294, 2013.

[19] Tiebiao Zhao, Brandon Stark, YangQuan Chen, Andrew L. Ray, and David Doll, "A detailed field study of direct correlations between ground truth crop water stress and normalized difference vegetation index (NDVI) from small unmanned aerial system (sUAS)," in *Unmanned Aircraft Systems (ICUAS), 2015 International Conference on*. IEEE, 2015, pp. 520–525.

[20] Geoffrey M. Smith and Edward J. Milton, "The use of the empirical line method to calibrate remotely sensed data to reflectance," *International Journal of Remote Sensing*, vol. 20, no. 13, pp. 2653–2662, 1999.

[21] Sunset, "Sunset climate zones: Central California," Website, http://www.sunset.com/garden/climate-zones/climate-zone-central-california.

[22] Richard G. Allen, Luis S. Pereira, Dirk Raes, Martin Smith, et al., "Crop evapotranspiration-guidelines for computing crop water requirements-FAO irrigation and drainage paper 56," *FAO, Rome*, vol. 300, no. 9, pp. D05109, 1998.

[23] A. Fulton, J. Grant, R. Buchner, and J. Connell, "Using the pressure chamber for irrigation management in walnut, almond, and prune," *Oakland: University of California Division of Agriculture and Natural Resources Publication*, vol. 8503, 2014.

[24] S. Stagakis, Victoria González-Dugo, Patricio Cid, M. L. Guillén-Climent, and Pablo J. Zarco-Tejada, "Monitoring water stress and fruit quality in an orange orchard under regulated deficit irrigation using narrow-band structural and physiological remote sensing indices," *ISPRS Journal of Photogrammetry and Remote Sensing*, vol. 71, pp. 47–61, 2012.

[25] David Doll, "The seasonal patterns of almond production," Website, 2009, http://thealmonddoctor.com/2009/06/22/the-seasonal-patterns-of-almond-production/.

[26] Brandon Stark and Tiebiao Zhao and YangQuan Chen, "An analysis of the effect of the bidirectional reflectance distribution function on remote sensing imagery accuracy from small unmanned aircraft systems," 2016, accepted for publication (ICUAS2016, Washington DC).